

Simulating polaron biophysics with Rydberg atoms

Marcin Płodzień¹, Tomasz Sowiński², Servaas Kokkelmans¹

¹ Department of Applied Physics, Eindhoven University of Technology, PO Box 513, 5600 MB Eindhoven, The Netherlands

² Institute of Physics, Polish Academy of Sciences, Aleja Lotników 32/46, PL-02668 Warsaw, Poland

Transport of excitations along proteins can be formulated in a quantum physics context, based on the periodicity and vibrational modes of the structures. Exact solutions are very challenging to obtain on classical computers, however, approximate solutions based on the Davydov ansatz have demonstrated the possibility of stabilized solitonic excitations along the protein. We propose an alternative study based on a chain of ultracold atoms. We investigate the experimental parameters to control such a quantum simulator based on dressed Rydberg atoms. We show that there is a feasible range of parameters where a quantum simulator can directly mimic the Davydov equations and their solutions. Such a quantum simulator opens up new directions for the study of transport phenomena in a biophysical context.

PACS numbers: 03.75.Hh, 32.80.Ee, 32.80.Qk, 42.50.p, 67.55.Hc, 67.85.d

Introduction.— Due to the remarkable progress in the understanding of molecular structures, life sciences succeed now in providing explanations of complex cell-biology phenomena, like light-harvesting complex [1]. Biological complexity of mesoscopic objects along with quantum behavior of the basic elements leads already to many unsolved questions awaiting comprehensive answers. Therefore, the interdisciplinary field of “quantum biology” is the natural area for combining quantum physical methods and tools to investigate, model and simulate biological systems on a mesoscopic level [2–4].

Some of the most fundamental biological processes such as protein folding, DNA repair, and muscle contractions, are directly related to the relaxation of the energy accumulated in chemical bonds into work. For example, many biological processes are powered by the energy obtained from the hydrolysis of adenosine triphosphate (ATP). On a physical level it can be viewed as a specific binding of the ATP molecule to a chosen site of the protein with energy equal to 0.49 eV. Since each site of the protein has a permanent dipole moment responsible for the energy excitation, one can treat an excitation as being well localized in the place where the ATP molecule is bound. Consequently, quite natural and important questions arise on the appropriate quantum description of the energy transport in such biological structures.

In 1970’s Davydov proposed a mechanism for the localization and transport of vibrational energy in the α -helix region of proteins [5–8]. The vibrational degrees of freedom are coupled to excitons forming an exciton-vibration localized state, called the Davydov’s soliton. Although this model has been used for a theoretical description of experimentally observed unconventional absorption bands in proteins [9, 10], a direct experimental evidence for forming the soliton is still missing.

The Davydov’s soliton is a subclass of richer phenomena called *polarons*, *i.e.*, excitations mediated by phonons which were originally introduced by Landau to describe deformations of the crystalline lattice caused by moving electron [11]. Landau’s model of polarons has been broadly studied theoretically as well as experimen-

tally in a condensed matter context [12] and in the last two decades it was successfully extended to different areas of ultra-cold physics: ultra-cold ions [13–19], polar molecules [20–24], ultra-cold Rydberg gases [25–27], and strongly-interacting ultracold Bose and Fermi gases [28–35].

In this letter we show that suitably prepared system of ultra-cold atoms off-resonantly coupled to Rydberg state [36–38] can serve as a dedicated quantum simulator of exciton-vibration interacting Hamiltonian and corresponding Davydov equations in semi-classical approximation. Being in an appropriate range of parameters, the quantum simulator can be used not only to obtain solutions of the Davydov’s equations but also to go *beyond* the Davydov model. Therefore, it can bring groundbreaking results for our understanding of biological phenomena.

The simulator.— To show that the atomic system can mimic behavior of the relevant biological molecule let us consider the system of ultra-cold atoms confined in a very deep one-dimensional optical lattice potential $V(x) = V_0 \sin^2(2\pi x/R_0)$ where each lattice site is occupied exactly by a single atom. We assume that the spatial dynamics of atoms is not completely frozen, *i.e.*, atoms may oscillate in vicinities of local minima with frequency $\omega_0 = \sqrt{2V_0\pi^2/mR_0^2}$. This motion is however quantized and therefore it is driven by a simple harmonic oscillator-like Hamiltonian:

$$\hat{\mathcal{H}}_{\text{vib}} = \sum_i \left(\frac{\hat{p}_i^2}{2m} + \frac{m\omega_0^2}{2} \hat{u}_i^2 \right) = \sum_i \hbar\omega_0 \hat{b}_i^\dagger \hat{b}_i, \quad (1)$$

where $\hat{u}_i = l_0(\hat{b}_i^\dagger + \hat{b}_i)/\sqrt{2}$ and $\hat{p}_i = i\hbar(\hat{b}_i^\dagger - \hat{b}_i)/(l_0\sqrt{2})$ are the position and momenta operators related to i -th atom, while operator \hat{b}_i annihilates vibrational excitation of i -th atom. Local motion defines a natural scale of length, $l_0 = \sqrt{\hbar/m\omega_0}$.

Besides spatial motion, each atom may exhibit changes of its internal state due to the long-range interactions between neighboring atoms. It is possible due to the off-resonant coupling of two different but degenerated internal Zeeman ground states $|g\rangle$ and $|g'\rangle$ to two precisely

selected, highly excited Rydberg states $|nS\rangle$ or $|nP\rangle$ with principal quantum number equal n and angular momentum equal 0 or \hbar , respectively [39, 40]. A first order perturbation analysis shows that this coupling results in a quite small admixture of a Rydberg state to the atomic ground states [41]. In consequence an atom can be found in one of the two dressed states:

$$|0\rangle \approx |g\rangle + \alpha_s |nS\rangle, \quad |1\rangle \approx |g'\rangle + \alpha_p |nP\rangle, \quad (2)$$

where amplitudes $\alpha_l = \Theta_l/2\Delta_l$ ($l \in \{s, p\}$) are determined by a total Rabi frequency of a driving field Θ_l and a total laser detuning Δ_l . In this basis of dressed states the dipole-dipole interaction between neighboring atoms C_3^{sp}/R^3 (R is a spatial distance between atoms), besides additional contribution to the energy gap between local states $|0_i\rangle$ and $|1_i\rangle$, may induce transitions (excitation hoppings) between internal states of neighboring atoms $|0_i\rangle|1_{i+1}\rangle \leftrightarrow |1_i\rangle|0_{i+1}\rangle$. In consequence, the excitation $|1\rangle$ can be effectively transported across the lattice. This effect is driven by the following Hamiltonian of internal motion of all atoms:

$$\hat{\mathcal{H}}_{\text{exc}} = \sum_i W_i \hat{a}_i^\dagger \hat{a}_i + \sum_i J_{i+1,i} (\hat{a}_{i+1}^\dagger \hat{a}_i + \hat{a}_i^\dagger \hat{a}_{i+1}), \quad (3)$$

where an annihilation operator of an excitation \hat{a}_i can be viewed as a local transition operator $|1_i\rangle\langle 0_i|$ between dressed Rydberg states. The spatial dependent parameters W_i and $J_{i+1,i}$ are related to the dipole-dipole forces induced by Rydberg dressing and they have a form [42, 43]:

$$W_i = \frac{\alpha^4 \hbar \Delta}{2} \left(\frac{1}{1 - \kappa(R_0 + u_{i+1} - u_i)^2} + \frac{1}{1 - \kappa(R_0 + u_i - u_{i-1})^2} \right),$$

$$J_{i+1,i} = \frac{\alpha^4 C_3^{sp}}{|R_0 + u_{i+1} - u_i|^3} \frac{1}{1 - \kappa(R_0 + u_{i+1} - u_i)^2}, \quad (4)$$

where $\kappa(R) = (C_3^{sp}/\hbar\Delta)/R^3$ and $\Delta = \Delta_s + \Delta_p$. In static situation, when all atoms are frozen, the energies W_i and $J_{i+1,i}$ are site-independent with values controlled by dipole-dipole interactions between neighboring atoms at fixed lattice spacing R_0 . However, due to the vibrational motion of atoms, these parameters are position dependent and they couple internal states of atoms with their motional degrees of freedom. In the lowest order approximation they can be written as $W_i = W_0 + g_W(u_{i+1} + u_{i-1})$, $J_{i+1,i} = -J_0 + g_J(u_{i+1} - u_i)$, where g_W and g_J are the appropriate Taylor expansion coefficients of (4) around R_0 . Moreover, since the vibrational motion is quantized, the parameters have an operator character when acting in the subspace of spatial motion of atoms. By inserting expanded W_i and $J_{i+1,i}$ to the Hamiltonian (3) one obtains so called Holstein-Su-Schrieer-Heeger Hamiltonian (HSSH) [44, 45]

$$\hat{\mathcal{H}} = \hat{\mathcal{H}}_{\text{exc}} + \hat{\mathcal{H}}_{\text{vib}}, \quad (5)$$

which is a model Hamiltonian for energy transport in biological systems. Our implementation can be regarded as a dedicated quantum simulator for this Hamiltonian to study such processes related to the α -helix protein.

The Rydberg dressing is responsible for the coupling between vibrational degrees of freedom of neighboring atoms. The resulting dressed soft-core interaction $\sim (R^6 + R_b^6)^{-1}$ [38], with R_b the Rydberg blockade radius, gives also rise to an additional energy shift. However, this shift is negligible compared to $\hbar\omega_0$, and therefore we omit it. In the following all energies are expressed in units of J_0 , and time is measured in units of \hbar/J_0 , *i.e.* we set $J_0 = \hbar = m = 1$.

Dynamical properties of the system.— A specific question related to the dynamics of the HSSH Hamiltonian is related to the transport of the excitation initially being localized on a chosen site K $|\Psi_0\rangle = \hat{a}_K^\dagger |\text{vac}\rangle$, or slightly delocalized on two neighboring sites $|\Psi_0\rangle = \frac{1}{\sqrt{2}}(\hat{a}_K^\dagger + \hat{a}_{K+1}^\dagger) |\text{vac}\rangle$, where $|\text{vac}\rangle$ is a vacuum state of the system fulfilling the condition $\hat{a}_i |\text{vac}\rangle = \hat{b}_i |\text{vac}\rangle = 0$ for any i . Experiments have shown that for specific parameters, a system prepared in these initial states evolves in such a way that the excitation does not spread across the protein. This is attributed to a specific ratio of the interactions of excitation and vibrational degrees of freedom, giving rise to a soliton. This spreading or non-spreading behavior can be extracted from information encoded in the time-dependent density profile $\rho_i(t) = \langle \Psi(t) | \hat{a}_i^\dagger \hat{a}_i | \Psi(t) \rangle$, where the state of the system at given time t can be formally written as

$$|\Psi(t)\rangle = \exp(-i\hat{\mathcal{H}}t) |\Psi_{\text{ini}}\rangle, \quad (6)$$

where $|\Psi_{\text{ini}}\rangle$ is one of the considered initial states. Temporal spreading of the excitation is simply captured by the width of the excitation wave packet $\sigma(t) = N [\sum_i \rho_i^2(t)]^{-1}$. This quantity takes the value $1/N$ for an excitation localized at exactly one lattice site and 1 for when it is fully delocalized. In principle, by analyzing the time-dependence of $\sigma(t)$ one can easily determine whether the excitation remains localized or whether it spreads across the system. Unfortunately, it is computationally quite demanding to find a solution of the evolution problem (6) due to the strong nonlinear quantum-mechanical coupling between excitation and vibrational degrees of freedom. Therefore generally the evolution of the system cannot be found exactly and some approximation methods have to be adopted.

The Davydov approach.— We discuss here the two-step Davydov approach [5], which results in a semiclassical description of the system. In the first step one assumes that the state of the system $|\Psi(t)\rangle$ can be well approximated by the product of two independent states $|\psi(t)\rangle$ and $|\phi(t)\rangle$ for excitation and vibrational degrees of freedom, respectively, $|\Psi(t)\rangle = |\psi(t)\rangle|\phi(t)\rangle$. Since the system is initially prepared in the state with precisely one excitation and the number of excitations is con-

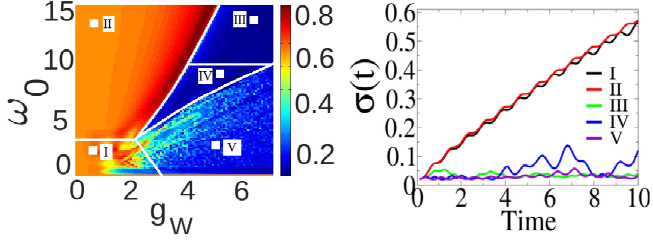


Figure 1. (Color online) Left panel: Maximal value of an excitation wave packet width $\max[\sigma(t)]$ as a function of ω_0 and g_W for vanishing coupling $g_J = 0$. A sharp crossover between non-spreading excitations (blue) and spreading excitation (dark red) is clearly visible. Different regions of the phase-diagram (bordered with white lines) correspond to a distinct nature of the exciton-vibration dynamics. Right panel: Evolution of the excitation width $\sigma(t)$ for different points on the phase diagram (marked as white squares on the left panel).

served, the state $|\psi(t)\rangle$ can be decomposed in the single-particle subspace, $|\psi(t)\rangle = \sum_i \psi_i(t) \hat{a}_i^\dagger |\text{vac}\rangle$, where time-dependent functions $\psi_i(t)$ play the role of probability amplitudes for finding an excitation at site i . Consequently $\rho_i(t) = |\psi_i(t)|^2$. The second step relays on a semiclassical treatment of the vibrational degrees of the system. In analogy to other quantum field theories, we assume that the state $|\phi(t)\rangle$ has classical features, *i.e.*, it can be well approximated by the product of independent coherent states: $|\phi(t)\rangle = \exp[-i \sum_i (u_i(t) \hat{p}_i - p_i(t) \hat{u}_i)] |\text{vac}\rangle$, where amplitudes $u_i(t)$ and $p_i(t)$ are expectation values of appropriate operators in the state $|\phi(t)\rangle$. Within these approximations it can be shown straightforwardly that the evolution equation (6) is equivalent to the set of coupled differential equations of the form:

$$i \frac{d\psi_i(t)}{dt} = -(\psi_{i+1} + \psi_{i-1}) + g_W(u_{i+1} - u_{i-1})\psi_i \quad (7a)$$

$$+ g_J[\psi_{i+1}(u_{i+1} - u_i) + \psi_{i-1}(u_i - u_{i-1})],$$

$$\frac{du_i(t)}{dt} = p_i(t), \quad (7b)$$

$$\frac{dp_i(t)}{dt} = -\omega_0^2 u_i(t) + g_W \omega_0 (|\psi_{i+1}|^2 - |\psi_{i-1}|^2) \quad (7c)$$

$$+ g_J \omega_0 [\psi_i^*(\psi_{i+1} - \psi_{i-1}) + \psi_i(\psi_{i+1}^* - \psi_{i-1}^*)].$$

These are the Davydov's type equations [5–8], which describe the dynamics of an excitation ψ_i coupled to a gradient of a classical field u_i forming an effective self-trapping potential. *Phase diagram.*— We perform a Semi-classical evolution of the system governed by Eqns. (7), which allows to observe spreading or non-spreading evolution of the excitation wave packet as function of the parameters $\{\omega_0, g_W, g_J\}$. The results can be visualized by the phase diagrams presented in Figs. 1 and 2. These diagrams are obtained by plotting the maximal value of the width of the excitation wave packet $\max[\sigma(t)]$ that is reached during the evolution up to maximal time $T_{\max} = 10\hbar/J_0$. All calculations are performed with

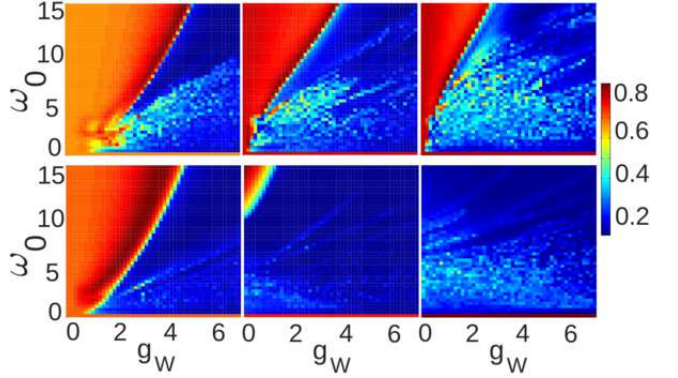


Figure 2. (Color scale) Maximal value of the wave packet width $\max[\sigma(t)]$ for different initial states $|\Psi_0\rangle$ and $|\tilde{\Psi}_0\rangle$ (top and bottom row, respectively) and different non-local interactions $g_J = \{0, 3, 5\}$ (appropriate columns from left to right). Note that strong enhancement of the non-spreading behavior takes place for stronger g_J and for a smeared out initial state.

$N = 50$ lattice sites and periodic boundary conditions. First, we focus on the case of a completely localized initial state $|\Psi_0\rangle$ for $g_J = 0$ (Fig. 1).

We qualitatively indicate five different regions on the phase diagram (left panel): (I) and (II) where the excitation is dressed by a cloud of vibrations and the excitation does spread; (III) where due to a dramatic reduction of the hopping amplitude $\sim J_0 e^{-(g_W/\omega_0)^2}$ the excitation is localized in its initial position [46]; (IV) where vibration energy and exciton-vibration coupling are larger than the hopping energy giving rise to Davydov-like soliton behavior; (V) where $g_W \gtrsim \omega_0$ corresponding to the Discrete Breathers-like behavior [47, 48]. Distinct behavior of the system is also visible in these selected areas in the time evolution of $\sigma(t)$ (right panel of Fig. 1).

This picture can be generalized to non-vanishing coupling g_J , which we investigate for the second initial state $|\tilde{\Psi}_0\rangle$ (Fig. 2). As can be seen, a slight delocalization of the initial together with non-local coupling g_J dramatically enhance the non-spreading behavior of the wave packet. It is a direct consequence of the non-local terms in (7).

Numerically exact approach.— The results obtained in the framework of the semi-classical Davydov approach can be supported by numerically exact dynamics governed by the many-body Hamiltonian (5). In this approach we represent the Hamiltonian $\hat{\mathcal{H}}$ as a matrix in the Fock basis spanned by many-body states $|i\rangle|m_1, \dots, m_N\rangle = \hat{a}_i^\dagger (\hat{b}_1^\dagger)^{m_1} \dots (\hat{b}_N^\dagger)^{m_N} |\text{vac}\rangle$, *i.e.*, states with an excitation located exactly at site i and with selected vibrational states m_i for all sites. An arbitrary state of the system can be expressed as an appropriate superposition of the basis states. Since the operator of a total number of vibrations in the system $\hat{N}_{\text{vib}} = \sum_i \hat{b}_i^\dagger \hat{b}_i$ does not commute with the Hamiltonian (5), therefore an exact evolution is obtained only in the limit where all Fock states are taken into account. In practice, for nu-

merical purposes, we assume that the total number of excitations cannot be larger than some well defined cut-off M . Then the results are treated as exact if increasing M does not change the outcome noticeably [49, 50]. Therefore, for given M , one can perform calculations only for a small range of parameters for which creations of vibrations is limited. It is worth noticing that numerical complexity grows exponentially with the cut-off M . For our parameters, $N = 50$ and $M = 3$ the size of the corresponding Hilbert space exceeds 1.1 million.

In Fig. 3 we show the time evolution of an initially localized excitation for $\omega_0 = 3$ and for three different values of the local coupling parameter $g_W = \{0.1, 0.75, 1.5\}$ ($g_J = 0$). It is clearly visible that for larger g_W the wave packet of the excitation becomes more stable and spreads less. This effect is directly reflected in the number of vibrational modes created, which can be seen in the right column of Fig. 3. One can observe that increasing fluctuations of the total vibrations in the system stabilize excitation.

Since we reached the limits of our computational method with this size of the Hilbert space, we cannot increase the coupling parameter further. From Fig. 3 it can be seen that the total number of vibrations for $g_W = 2$ is close to the limiting cut-off. At the same time, however, this is a strong argument for employing a quantum simulator, such as proposed in this letter, to validate the predictions of the semi-classical.

Experimental parameters.— The numerical predictions for the model described by the Hamiltonian (5) are quite general. For a quantum simulator we consider ^{87}Rb atoms confined in an optical lattice determined by lattice spacing $R_0 = 1 \mu\text{m}$ and $V_0 = 100E_R$ (recoil energy $E_R = 2\pi^2\hbar^2/mR_0^2$) [39], i.e., the local trap frequency is equal to 6.2 kHz. We assume Rydberg states with principal quantum number $n = 50$ for which $C_3^{sp} = 3.224 \text{ GHz } \mu\text{m}^3$ [51]. We choose the dressing parameters as $\alpha = 0.015$ and $\Delta/2 = \Delta_s = \Delta_p = 2.5 \text{ GHz}$. With these values, the system mimics the Hamiltonian (5) with dimensionless parameters $\omega_0 = 4.7$, $g_W = 5.6$, and $g_J = 5.6$. These parameters can be easily tuned since they strongly depend on the lattice spacing R_0 and on the set of laser detunings. In this way a large and interesting area of the phase diagrams presented in Fig. 2 can be covered. The estimated lifetime of Rydberg atoms excited to states with $n = 50$ is $\tau_S = 65 \mu\text{s}$ and $\tau_P = 86 \mu\text{s}$ [52]. The effective of a dressed state is scaled by a factor α^{-2} and as a consequence a sufficiently long time is obtained to form and observe non-spreading excitation behavior.

It is worth noting that also other experimental realizations, based for example on Rydberg microtrap arrays [53] instead of an optical lattice, can be considered as proper candidates for simulating this system.

Conclusions.— We show that a system of ultracold Rydberg atoms confined in a one-dimensional optical lattice may serve as a dedicated quantum simulator for exciton-vibration dynamics, which is a subclass of polaron dynamics. Since effective parameters of the resulting model

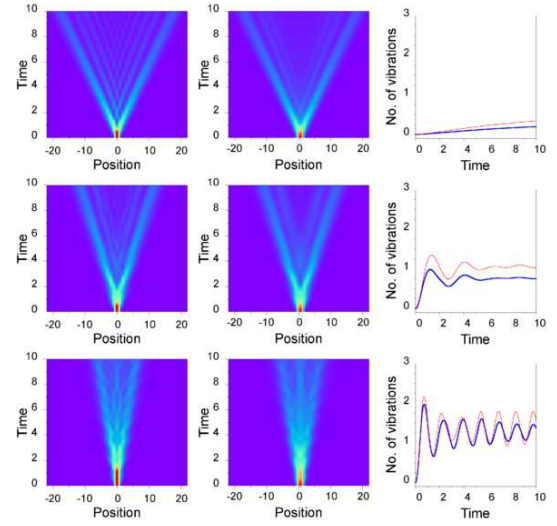


Figure 3. Exact evolution of the excitation wave packet governed by the Hamiltonian (5) for the initial state $|\Psi_0\rangle$ (left column) and $|\tilde{\Psi}_0\rangle$ (middle column). The right column shows the total number of vibrations \tilde{N}_{vib} created in the system during the evolution (thick blue and thin red line for left and middle column, respectively). Consecutive rows corresponds to different local couplings $g_W = \{0.1, 0.75, 1.5\}$. All calculations performed for $g_J = 0$ and $\omega_0 = 3$. Note that for stronger interactions evident stabilization of the excitation density profile, along with increasing number of created vibrations, is observed.

can be easily tuned, the system can be used to mimic transport of excitation in biologically active proteins and to perform full quantum mechanical tests of the semi-classical predictions.

Acknowledgements.— This work was supported by the (Polish) National Science Center Grant No. 2016/22/E/ST2/00555 (TS), by the Foundation for Fundamental Research on Matter (FOM), by the Netherlands Organisation for Scientific Research (NWO), and by the European Union H2020 FET Proactive project RySQ (grant N. 640378).

[1] M. Sarovar, A. Ishizaki, G. Fleming, and K. B. Whaley *Nature Physics*, vol. 6, p. 462, 2010.
[2] M. Arndt, T. Juffmann, and V. Vedral *HFSP Journal*, vol. 3, no. 6, pp. 386–400, 2009.
[3] S. Huelga and M. Plenio *Contemporary Physics*, vol. 54, no. 4, 2013.
[4] Z. qi Yin and T. Li *Contemporary Physics*, vol. 0, no. 0, pp. 1–21, 2016.

[5] A. Davydov *Phys. Stat. Sol.*, vol. 36, p. 211, 1969.

[6] A. Davydov *J. Theor. Biol.*, vol. 38, p. 559, 1973.

[7] A. Davydov *Phys. Stat. Sol.*, vol. 59, p. 465, 1973.

[8] K. N. I. Davydov A.S. *Zh. Eksp. Teor. Fiz.*, vol. 71, p. 1090, 1976.

[9] G. Careri, U. Buontempo, F. Carta, E. Gratton, and A. C. Scott, “Infrared absorption in acetanilide by solitons,” *Phys. Rev. Lett.*, vol. 51, pp. 304–307, 1983.

[10] G. Careri, U. Buontempo, F. Galluzzi, A. C. Scott, E. Gratton, and E. Shyamsunder, “Spectroscopic evidence for davydov-like solitons in acetanilide,” *Phys. Rev. B*, vol. 30, pp. 4689–4702, 1984.

[11] L. D. Landau *Z. Phys.*, vol. 3, p. 664, 1933.

[12] D. J. Alexandrov, A.S., *Advances in Polaron Physics*. Springer-Verlang, 2010.

[13] D. Porras and J. I. Cirac *Phys. Rev. Lett.*, vol. 92, p. 207901, 2004.

[14] M. Mller, L. Liang, I. Lesanovsky, and P. Zoller *New Journal of Physics*, vol. 10, p. 093009, 2008.

[15] K. Kim, M.-S. Chang, R. Islam, S. Korenblit, L.-M. Duan, and C. Monroe *Phys. Rev. Lett.*, vol. 103, p. 120502, 2009.

[16] J. P. Hague and C. MacCormick *New Journal of Physics*, vol. 14, p. 033019, 2012.

[17] A. Mezzacapo, J. Casanova, L. Lamata, and E. Solano *Phys. Rev. Lett.*, vol. 109, p. 200501, 2012.

[18] V. M. Stojanović, T. Shi, C. Bruder, and J. I. Cirac *Phys. Rev. Lett.*, vol. 109, p. 250501, 2012.

[19] L. Lamata, A. Mezzacapo, J. Casanova, and E. Solano *EPJ Quantum Technology*, vol. 1, p. 9, 2014.

[20] J. Prez-Ros, F. Herrera, and R. V. Krems *New Journal of Physics*, vol. 12, no. 10, p. 103007, 2010.

[21] F. Herrera, M. Litinskaya, and R. V. Krems *Phys. Rev. A*, vol. 82, p. 033428, 2010.

[22] F. Herrera and R. V. Krems *Phys. Rev. A*, vol. 84, p. 051401, 2011.

[23] W. Li and I. Lesanovsky *Phys. Rev. Lett.*, vol. 108, p. 023003, 2012.

[24] F. Herrera, K. W. Madison, R. V. Krems, and M. Berciu *Phys. Rev. Lett.*, vol. 110, p. 223002, 2013.

[25] J. P. Hague and C. MacCormick *Phys. Rev. Lett.*, vol. 109, p. 223001, 2012.

[26] J. P. Hague, S. Downes, and P. E. MacCormick, C. and Kornilovitch *Journal of Superconductivity and Novel Magnetism*, vol. 27, p. 937, 2014.

[27] D. Schöngleber, A. Eisfeld, M. Genkin, S. Whitlock, and S. Wüster *Phys. Rev. Lett.*, vol. 114, no. 7, p. 123005, 2015.

[28] A. Schirotzek, C.-H. Wu, A. Sommer, and M. W. Zwierlein *Phys. Rev. Lett.*, vol. 102, p. 230402, 2009.

[29] M. Koschorreck, D. Pertot, E. Vogt, B. Frölich, M. Feld, and M. Köhl *Nature*, vol. 485, p. 619, 2012.

[30] M.-G. Hu, M. J. Van de Graaff, D. Kedar, J. P. Corson, E. A. Cornell, and D. S. Jin *Phys. Rev. Lett.*, vol. 117, p. 055301, 2016.

[31] N. B. Jørgensen, L. Wacker, K. T. Skalmstang, M. M. Parish, J. Levinsen, R. S. Christensen, G. M. Bruun, and J. J. Arlt, “Observation of attractive and repulsive polarons in a bose-einstein condensate,” *Phys. Rev. Lett.*, vol. 117, p. 055302, 2016.

[32] M. M. Parish and J. Levinsen *Phys. Rev. B*, vol. 94, p. 184303, 2016.

[33] E. Nakano, H. Yabu, and K. Iida *Phys. Rev. A*, vol. 95, p. 023626, 2017.

[34] E. A. D. Fabian Grusdt, Gregory E. Astrakharchik *arXiv:1704.02606*, 2017.

[35] F. Scazza, G. Valtolina, P. Massignan, A. Recati, A. Amico, A. Burchianti, C. Fort, M. Inguscio, M. Zaccanti, and G. Roati *Phys. Rev. Lett.*, vol. 118, p. 083602, 2017.

[36] N. Henkel, R. Nath, and T. Pohl *Phys. Rev. Lett.*, vol. 104, p. 195302, 2010.

[37] J. E. Johnson and S. L. Rolston *Phys. Rev. A*, vol. 82, p. 033412, 2010.

[38] J. Honer, H. Weimer, T. Pfau, and H. P. Büchler *Phys. Rev. Lett.*, vol. 105, p. 160404, 2010.

[39] T. Macrì and T. Pohl *Phys. Rev. A*, vol. 89, p. 011402, 2014.

[40] J. Zeiher, R. van Bijnen, P. Schauss, S. Hild, J. Choi, T. Pohl, I. Bloch, and C. Gross *Nature Phys.*, vol. 12, p. 1095, 2016.

[41] J. Honer, H. Weimer, T. Pfau, and H. P. Büchler *Phys. Rev. Lett.*, vol. 105, p. 160404, 2010.

[42] S. Wüster, C. Ates, A. Eisfeld, and J. M. Rost *New Journal of Physics*, vol. 13, p. 073044, 2011.

[43] M. Genkin, S. Wüster, S. Möbius, A. Eisfeld, and J. Rost *J. Phys. B*, vol. 47, p. 095003, 2014.

[44] T. Holstein *Ann. Phys.*, vol. 8, p. 325, 1959.

[45] W. P. Su, J. R. Schrieffer, and A. J. Heeger *Phys. Rev. Lett.*, vol. 42, pp. 1698–1701, 1979.

[46] F. K. Campbell, D.K. *Phys. Rev. B*, vol. 26, p. 6862, 1982.

[47] S. Flach and C. Willis, “Discrete breathers,” *Physics Reports*, vol. 295, no. 5, pp. 181 – 264, 1998.

[48] B. Juanico, Y.-H. Sanejouand, F. Piazza, and P. De Los Rios *Phys. Rev. Lett.*, vol. 99, p. 238104, 2007.

[49] T. Sowiński, M. Gajda, and K. Rzżewski *Europhys. Lett.*, vol. 113, p. 56003, 2016.

[50] J. Dobrzyniecki and T. Sowiński *Eur. Phys. J.*, vol. 70, p. 83, 2016.

[51] S. Weber, C. Tresp, H. Menke, A. Urvoy, O. Firstenber, H. Büchler, and S. Hofferberth *arXiv:1612.08053*, 2016.

[52] I. I. Beterov, I. I. Ryabtsev, D. B. Tretyakov, and V. M. Entin *Phys. Rev. A*, vol. 79, p. 052504, 2009.

[53] V. Y. F. Leung, A. Tauschinsky, N. J. van Druten, and R. J. C. Spreeuw *Quantum Information Processing*, vol. 10, no. 6, p. 955, 2011.